



Universiteit  
Leiden  
The Netherlands

## Origami metamaterials : design, symmetries, and combinatorics

Dieleman, P.

### Citation

Dieleman, P. (2018, October 16). *Origami metamaterials : design, symmetries, and combinatorics*. *Casimir PhD Series*. Retrieved from <https://hdl.handle.net/1887/66267>

Version: Not Applicable (or Unknown)

License: [Licence agreement concerning inclusion of doctoral thesis in the Institutional Repository of the University of Leiden](#)

Downloaded from: <https://hdl.handle.net/1887/66267>

**Note:** To cite this publication please use the final published version (if applicable).

Cover Page



Universiteit Leiden



The handle <http://hdl.handle.net/1887/66267> holds various files of this Leiden University dissertation.

**Author:** Dieleman, P.

**Title:** Origami metamaterials : design, symmetries, and combinatorics

**Issue Date:** 2018-10-16

# Origami Metamaterials: Design, Symmetries, and Combinatorics

Proefschrift

ter verkrijging van  
de graad van Doctor aan de Universiteit Leiden,  
op gezag van Rector Magnificus prof. mr. C.J.J.M. Stolker,  
volgens besluit van het College voor Promoties  
te verdedigen op dinsdag 16 oktober 2018  
klokke 15.00 uur

door

**Peter Dieleman**  
geboren te Rotterdam  
in 1990

PROMOTOR

Prof. dr. M.L. van Hecke

PROMOTIECOMMISSIE

Dr. A. Murugan (*Universiteit van Chicago, Chicago, VS*)

Dr. ir. J.T.B. Overvelde (*AMOLF, Amsterdam*)

Prof. dr. P.M. Reis (*EPFL, Lausanne, Zwitserland*)

Prof. dr. J. Aarts

Prof. dr. ir. S.J. van der Molen

Prof. dr. H. Schiessel

Casimir PhD Series, Delft-Leiden, 2018-32

ISBN 978-90-8593-361-8

An electronic version of this thesis can be found at [openaccess.leidenuniv.nl](http://openaccess.leidenuniv.nl)

Supporting images and files can be found at [http://bit.ly/supplemental\\_files](http://bit.ly/supplemental_files) or via the QR codes printed in the margin of this thesis.

The work described in this thesis was supported by the Stichting voor Fundamenteel Onderzoek der Materie (FOM), presently part of NWO.

The cover shows one of the combinatorial fold patterns described in this thesis (p. 60). Depending on how you fold it, this crease pattern folds up into the shape of the Greek letter ' $\alpha$ ', or the into the shape of the Greek letter ' $\omega$ '.





---

# Contents

---

<b>1</b>	<b>Introduction</b>	<b>1</b>
1.1	Origami . . . . .	1
1.2	Rigid Folding . . . . .	5
1.2.1	Single Crease . . . . .	5
1.2.2	Rigidly Folding Vertices . . . . .	6
1.2.3	4-Vertex Fold Patterns . . . . .	8
1.3	This Thesis . . . . .	9
<b>2</b>	<b>Discrete Origami Tiles</b>	<b>11</b>
2.1	Introduction . . . . .	11
2.2	Rigid Folding Conditions . . . . .	12
2.3	Combinatorial Loop Condition . . . . .	13
2.4	Tiles . . . . .	16
2.5	Bricks . . . . .	18
2.6	Summary and Outlook . . . . .	23
<b>3</b>	<b>Classification of Tile Patterns</b>	<b>25</b>
3.1	Introduction . . . . .	25
3.2	Triplet Completion and Classification . . . . .	27
3.3	Counting Multiplicity of Tilings . . . . .	29
3.4	Counting Supplementation Patterns . . . . .	36
3.5	Counting Folding Branches . . . . .	44
3.6	Summary and Outlook . . . . .	48

## CONTENTS

---

<b>4</b>	<b>Rational Design of Origami Patterns</b>	<b>51</b>
4.1	Introduction . . . . .	51
4.2	Space-Filling Tilings . . . . .	52
4.3	Designing Origami Strips with One Target Shape . . . . .	53
4.4	Designing Origami Sheets with Two Target Shapes . . . . .	57
<b>5</b>	<b>Multistability of Non-Flat Vertices</b>	<b>63</b>
5.1	Introduction . . . . .	63
5.2	Non-Flat 4-Vertices . . . . .	64
5.2.1	Phenomenology . . . . .	64
5.2.2	Theoretical Energy Curves . . . . .	69
5.3	3D Printed Tristable Vertices . . . . .	71
5.4	Experimental Results . . . . .	74
5.4.1	Tristable Vertex: Qualitative Results . . . . .	74
5.4.2	Experimental Protocol for Torsion Experiments . . . . .	75
5.4.3	Torsion Experiments - Results . . . . .	79
5.4.4	Experimental Energy Curves . . . . .	88
5.4.5	Vertex Pop-Through . . . . .	92
5.5	Conclusion . . . . .	98
<b>A</b>	<b>Fold Angles</b>	<b>99</b>
<b>B</b>	<b>4-Vertex as a Spherical Mechanism</b>	<b>103</b>
	<b>Samenvatting</b>	<b>115</b>
	<b>Summary</b>	<b>119</b>
	<b>Publication List</b>	<b>123</b>
	<b>Curriculum Vitae</b>	<b>125</b>
	<b>Acknowledgments</b>	<b>127</b>



# INTRODUCTION

---

## 1.1 Origami

Folding paper for decorative purposes is an art that seems to have developed separately in different parts of the world [1, 2], but is now known worldwide by the Japanese word ‘origami’, meaning: ‘folding paper’. Origami in Japan is thought to originate from the folding of ceremonial wrappers during the 14th century [1], and evolved in complexity over the subsequent centuries (Fig. 1.1.A). Folding paper in Europe seems to stem from the 16th century, as a way to make baptismal certificates [1] (Fig. 1.1.B), and was later also used for decorative purposes, for example, to elaborately fold napkins (Fig. 1.1.C). Up until 1854, when the United States and Japan signed the Kanagawa treaty [6], there was very little mixing of the Western and Japanese traditions of paper folding [1, 2]. The modern day interpretation of ‘origami’ is a result of the mixing of these two traditions after the modernization of Japan during the second half of the 19th century [1].

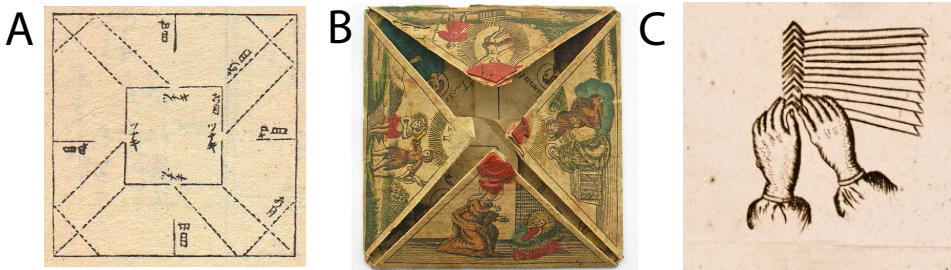


FIGURE 1.1: (A) Origami Fold pattern from a 1797 Japanese book [3]. (B) German ‘Patenbrief’ (baptism certificate), dated 1769. (C) Instructions on decoratively folding napkins from a 1754 Dutch cooking book [4]. Figures from [5].

In the 1950s, the development of a standard way to draw origami diagrams allowed for more efficient sharing of origami models [7]. At the same time, mathematicians started to get interested in the mathematics behind paper folding, starting with the 1949 book ‘Geometric Tools’ [8]. Since then, mathematicians have found a variety of necessary conditions which crease patterns should satisfy in order to fold, first at the level of single vertices [9, 10], and later at the level of folding patterns [11–16].

Building on these mathematical rules, and benefiting from the increasing popularity of computers, emerged the field of ‘computational origami’. The first major breakthrough in this field was an algorithm named ‘Treemaker’ developed by Robert Lang, first released in 1993 [17]. This program finds a two-dimensional fold pattern for a given three-dimensional shape, allowing for the design of very complex origamis. A different and more sophisticated algorithm was developed by Tomohiro Tachi [18, 19]. An example of the capability of this latter algorithm is shown in Fig. 1.2.A, where we depict a complicated two-dimensional folding pattern designed to fold into the shape of a ‘Stanford Bunny’, containing 374 triangles [19]. Fig. 1.2.B displays a three-dimensional, manually folded version of this crease pattern, made out of paper.

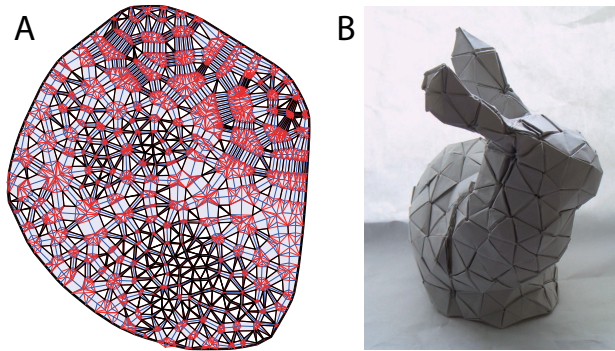


FIGURE 1.2: (A) 2D crease pattern, containing 374 triangles, designed to fold into the shape of a ‘Stanford Bunny’. (B) Paper folded into the shape of a Stanford Bunny according to the crease pattern in (A). Figure adopted from [19].

The most recent wave of interest in origami comes from the fields of physics and engineering. This interest can be traced back to the 1960s, when engineers started to consider origami based materials for structural

applications. Specifically, various patents were filed for so called ‘folded sandwich core’ panels [20, 21]. These panels consist of a sheet of material folded in a ‘double corrugated shape’, glued onto a skin on the top and the bottom (Fig. 1.3). Designs such as these promised to outperform ‘classic’ honeycomb sandwich core panels in terms of transversal shear stiffness for the same weight [22, 23], but proved impractical at the time, due to the sensitivity to fabrication imperfections [24, 25]. However, advances in fabrication processes have renewed interest in these materials, giving rise to a large number of experimental and numerical studies [23].

More recently, it has been shown that origami inspired materials can exhibit a variety of exotic properties, ranging from a negative Poisson’s ratio [26], to tuneable stiffness [27], to multistability [28]. In addition, origami can serve as a low-cost manufacturing platform for the fabrication of simple robots [29–31]. Here, we will show some examples of these exotic properties.

One example is the folded core of the panel in Fig. 1.3, which is also shown in Fig. 1.4.A. Here it is demonstrated that this sheet has a negative 2D-Poisson’s ratio, as it shrinks in both planar directions simultaneously. This property can be harnessed by stacking multiple sheets to make a 3D origami structure that can contract (or expand) in all three orthogonal directions simultaneously, which is impossible with a regular (positive Poisson’s ratio) solid [26, 32]. This pattern is now called the “Miura-ori” pattern, named after K. Miura, who proposed it as an effective way to pack and deploy large membranes for space-flight, as it can unfold with a single continuous motion, using a minimal amount of motors [33].

This Miura pattern –as well as derivatives– have since been extensively

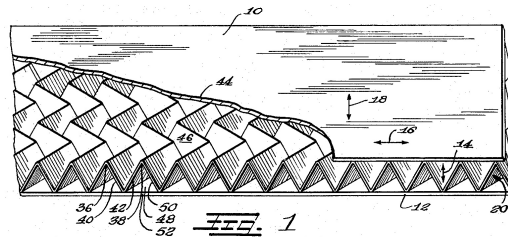


FIGURE 1.3: Patent filing for a folded core sandwich panel, figure adapted from [20].

studied, and a host of other interesting properties have been discovered; such as multistability [28], arbitrary shape change [34], and the ability to reversibly program the stiffness of a sheet [27, 35]. For example, in [27] it is shown that it is possible to pop-through a single unit cell of the Miura pattern in its folded configuration, introducing a so-called ‘pop-through defect’. The presence of these pop-through defects can change the compressive stiffness of the sheet, as the fold pattern is locally frustrated. In some cases however, two adjacent pop-through defects can interact in such a way as to generate a lattice vacancy. These lattice vacancies give rise to various crystallographic structures, such as grain boundaries, and edge dislocation – an example of the latter is shown in Fig. 1.7.B [27].

Additionally, fold patterns seem to be ubiquitous in nature, appearing naturally in leaves [37–39], insect wings [40, 41], and in embryonic gut tissue in chicks [36]. This natural occurrence is attributed to the material growing within a constrained environment [38, 42]. For example, when the gut-tube of an embryonic chick is developing it is initially smooth, but when the development of circumferentially oriented muscle tissue starts, inward buckling of the tube prompts the formation of ridges in the longitudinal direction. A second layer of *longitudinally* oriented muscle then starts to develop several days later, after which the longitudinal ridges themselves buckle into parallel zigzags [43], leading to the pattern shown in Fig. 1.4.C.

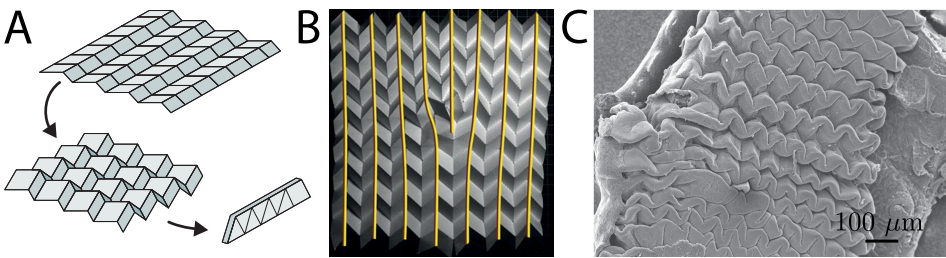


FIGURE 1.4: (A) A Miura-ori pattern shows auxetic (negative Poisson’s ratio) behavior. (B) Multiple pop-through defects in a column of a Miura-ori sheet give rise to an edge dislocation [27]. (C) SEM picture of turkey gut, showing a fold structure resembling the Miura-ori pattern. Panel (A) adapted from [32], panel (B) adapted from [27], panel (C) adapted from [36].



## 1.2 Rigid Folding

In this section I will explain the concept of *rigid* folding, which is central to understanding the work in this thesis. In addition, I will explain what this means in the case of a single 4-vertex, and for patterns consisting of multiple 4-vertices.

### 1.2.1 Single Crease

The simplest possible origami pattern that we can study is a single crease, which already turns out to have interesting mechanics. When applying a crease to a piece of material, we plastify some of the bonds in the paper, such that their rest positions are no longer flat. When we then pull the material outward we effectively open the crease, which then acts as a torsional spring. Additionally, the sheet itself may deform and bend. The length scale that determines which of these elastic effects dominates, is called the origami length scale [44]:

$$L^* = \frac{B}{\kappa}. \quad (1.1)$$

Here  $B$  is the bending modulus,  $B = Eh^3/12(1 - \nu^2)$ ,  $E$  is the Young's modulus,  $\nu$  is the Poisson's ratio, and  $h$  the thickness of the material.  $\kappa$  is defined as the effective torsional stiffness of the crease. Based on the energy stored in a single crease, it can be shown that the torsional stiffness should scale roughly as  $\kappa = B/h$  [45]. The length scale  $L^*$  therefore linearly increases with the thickness of the material  $h$ . Experiments in [44] for Mylar sheets show that there is a large separation of scales between  $h$  and  $L^*$ .

This separation of scales can be explained by a separation of scales between the Young's modulus of the material, which sets  $B$  in Eq. 1.1, and the yield stress  $\sigma_Y$ , which sets  $\kappa$  in Eq. 1.1. The existence of this difference allows for the following two scenarios: sheets with a fold pattern where the length of the creases,  $l$ , is larger than  $L^*$ , and sheets whose crease length  $l$  is smaller than  $L^*$ . This difference can be demonstrated by folding a sheet of material into an accordion shape, such as shown in Fig. 1.5. In the case  $l > L^*$  extending the sheet will not change the angle between the plate very much from its rest angle ( $\phi \approx \phi_0$ ), but instead will bend the plates (Fig. 1.5.B). In the case  $l < L^*$  the deformation is concentrated in the crease,

which acts as an approximately linear torsional spring, and the panels stay almost completely straight (Fig. 1.5.D) [44]. In the scenario where  $l < L^*$  we can therefore approximate a fold pattern by a set of hinges, dressed with torsional springs, connecting rigid plates – this is the rigid folding limit.

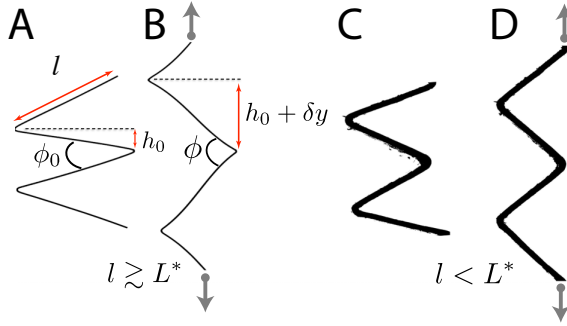


FIGURE 1.5: Side view of two sheets of Mylar with thickness  $h = 130 \mu\text{m}$ , folded into an accordion shape (A,C), and extended by pulling on the top and bottom (B,D). (A) Rest state with  $l = 2.5 \text{ cm}$ . (B) Deformed state. (C) Rest state with  $l = 0.6 \text{ cm}$ . (D) Deformed state.  $L^* \approx 2.5 \text{ cm}$ . Figure adapted from [44].

### 1.2.2 Rigidly Folding Vertices

The fold pattern shown in Fig. 1.5 is a very simple one, consisting of parallel lines. Most fold patterns are more complicated than this, and also contain *vertices*, i.e. points where multiple folds come together (see Fig. 1.4.A,B). It is therefore important to understand what happens at these vertices. If we assume the rigid folding condition, where the plates are perfectly rigid, we can use 3D Maxwell-Calladine constraint counting to count the number of floppy modes of a single vertex [46, 47].

In the case of a vertex where three lines come together (shown in blue in Fig. 1.6.A), we count  $4 \times 3 = 12$  degrees of freedom (d.o.f.) for the 4 points in 3D space. These points cannot freely move, but are constrained by  $3 \times 1 + 3 \times 1 = 6$  constraints: the 3 black bonds (which represent the fold lines), and 3 gray bonds (representing the rigid plates), which each represent one constraint. In total we therefore have  $12 - 6 = 6$  degrees of freedom. These correspond to the 6 degrees of freedom (rotation and